

Structural Controls and Slip Tendency in the Chiweta Geothermal Zone: Northern Part of the Malawi Rift, Africa.

Estefanny Dávalos-Elizondo^{1*} and Daniel A. Laó-Dávila¹

¹ Boone Pickens School of Geology, Oklahoma State University, 105 Noble Research Center, Stillwater, OK 74078-3031, USA. edavalo@okstate.edu*

Keywords

Malawi Rift, Hot Spring, Accommodation Zone, Mohr Circle, Slip Tendency, Stress State, Favorable Structures, Pore fluid pressure

ABSTRACT

The Chiweta hot spring is one of the hottest hot spring with reservoir temperatures estimated at ~200 °C by cation geothermometers. The Chiweta hot spring is located in the northwest of the Malawi Rift, where volcanic activity is not present. However, it is suggested that the Chiweta's geothermal system is strongly controlled by faults.

We used Shuttle Radar Topography Mission Digital Elevation Model to map brittle structures on the surface and characterize the favorable structures that may control the storage of the Chiweta geothermal system. Our results show that structures NW-SE, NE-SW and N-S are predominant in the Chiweta area. We suggest that the accommodation zone between the Livingstone and Usysia faults controls the Chiweta's geothermal system.

Additionally, we performed the Mohr circle and slip tendency analysis to identify the main orientations of potential active segments along faults capable to transport the geothermal fluids. Our results show that ~NW-SE and ~N-S pre-existing structures of Quaternary ages with ~60° dip have high slip tendency. These structures are likely the main pathways of the hot fluids to the surface in the Chiweta geothermal zone. Whereas the ~NE-SW pre-existing structures of Paleo-Mesozoic age have moderate slip tendency and are possible confining structures of the geothermal system.

The first stress state shows a preferential failure plane oriented ~332°/56°, the second is oriented ~167°/53°, and the last one is oriented ~176°/63°. The pore fluid pressure increases the slipping tendency and it is probably higher in areas where fluids are present. We concluded that all these intersections and overlapping structures are assisting permeability in the Chiweta zone. Our results and future studies could help to identify the most promising drilling targets for exploration wells to continue geothermal energy development in this country.

1. Introduction

The Malawi Rift is a magma-poor continental rift system located in the Western branch (Fig. 1A) of the East African Rift System (EARS). A geothermal anomaly through the continental crust under the Malawi Rift is supported by high heat flow values between 77 to 120 mW/m² (Von Herzen & Vacquier, 1967; Njinju et al., 2015). The only Quaternary volcano in the Malawi Rift is the Rungwe volcanic complex located in the northern part. Likewise, recent seismic tomographic models in the Malawi Rift show lower P-S waves velocities that were interpreted as a super-plume mantle beneath the Rungwe volcano complex, and magma intrusions at depth southward of Malawi Rift (Grijalva et al., 2018; Wang et al., 2019). In addition, more than 55 hot springs along the rift (Gondwe et al., 2015) evidence the presence of geothermal systems at depth. Regardless of this evidence, Malawi is in the first geothermal exploration stages without geothermal capacity installed yet.

Geothermal exploration studies have focused on understanding the geochemistry of hot springs across Malawi (e.g. Dixey, 1927; Bloomfield, 1965; Bloomfield & Garson, 1965; Harrison & Chapusa, 1975; Ray, 1975; Dulanya, 2006; Dulanya et al., 2010; Msika et al., 2014; Kalebe, 2017; Atekwana et al., 2015; and Dávalos-Elizondo et al., 2018). Dávalos-Elizondo et al. (2018) carried out geothermometry calculations to estimate reservoir temperatures of 27 hot springs along the rift (Fig. 1B). The geothermometry results reported by these authors showed the highest reservoir temperatures of ~200 °C in the Chiweta hot springs located in the northern part of the rift. Furthermore, the geothermometer results show that the Chiweta geothermal zone has at least medium enthalpy. Geothermal systems associated with the hot springs in Malawi are expected to be fault controlled (e.g. Atekwana et al., 2015; Dávalos-Elizondo et al., 2018).

There are several studies about fault controlled geothermal systems (e.g. Basin and Range province, USA) that support that faulting increases permeability and provides geothermal fluids circulation pathways (e.g. Barton et al., 1995; Evans et al., 1997; Blackwell et al., 1999; Faulds et al., 2006; Faulds et al., 2011; Siler and Faulds., 2013; Faulds et al., 2013). Faulds et al. (2011) identified different favorable structures in the Basin and Range province, such as termination of a major normal faults, step-over or relay ramp in a normal fault zone, accommodation zones, antithetic normal fault, fault intersections, pull apart basins, strike-slip fault zones, displacement transfer zones, etc. It is important to understand which and how favorable structures control geothermal systems in the Malawi Rift to continue with the geothermal energy development. These favorable structures and their relationship with heat flow, magmatic intrusions, hot springs, fluid pathways, and extension could help to identify promising drilling targets for exploration wells.

The goal of this study is to identify the main favorable structures with the potential to control the geothermal fluid pathways in the surface of the Chiweta geothermal zone. Our specific objectives are to characterize the orientation of major faults, fractures, and foliations. Then, compare them within the current stress field to determine which planes (strike/dip) within a geothermal system are most likely to slip and transport the hot fluids. To accomplish our goal, remote sensing techniques were used to map brittle structures of the shallow crust and identify the main different orientations in our study area. Subsequently, slip tendency analysis was performed to identify the most favorable structures to transport the fluids in the Chiweta area.

2. Tectonic setting

The Western branch is a volcanic poor region of the EARS (Fig. 1A), which has been affected by repeated rifting cycles since the Late Paleozoic (McConnell, 1972; Delvaux, 2001). It is characterized by asymmetric basins (< 100 km wide) flanked by major faults, usually with alternating polarity (e.g., Rosendahl et al., 1992). Most of the seismic activity of the EARS is focalized in the Western branch (Roberts et al., 2012). Several studies have shown that the increase in seismic activity is related with early stages of rifting, where the extension is accommodated by displacement along major faults before it is transferred to the hanging wall due to magma intrusions (e.g., Kolawole et al., 2018; Calais et al., 2008; Ebinger & Casey, 2001; Goldsworthy & Jackson, 2001).

The Malawi Rift is part of the Western branch and is characterized by an old (Precambrian rocks), cold, and thick lithosphere (~41-45 km; Njinju et al., 2015) associated with localized strain along major faults (Fig. 1B). It is ~900 km in length from the Rungwe Volcanic Complex (RVC) to the Dombe and Urema grabens in Mozambique (Ebinger, 1989; Ring et al., 1994; Chorowicz, 2005; Laó-Dávila et al., 2015). Lake Malawi occupies most of the rift (Fig. 1B) and extends for ~650 km with width ranges from 75 to 50 km and a maximum depth of ~ 7 km (McCartney & Scholz, 2016; Grijalva et al., 2018).

This rift is developed within Proterozoic orogenic belts following the NW-trend of the Paleoproterozoic Ubendian Belt (Fig. 1B) overprinted by the actual N-S-trend of the Quaternary rift (Laó-Dávila et al., 2015). These spatial and orientation relationships suggest that large inherited lithospheric structure controls the evolution of some regions of the rift (e.g., Corti et al., 2007; Laó-Dávila et al., 2015; Dawson et al., 2018), which has a current extension oriented E-W indicated by focal mechanism in the northern area (e.g. Biggs et al., 2010; Saria et al., 2014). Ebinger et al. (1993) used K-Ar and $^{40}\text{Ar}/^{39}\text{Ar}$ to determine ages of volcanic rocks and concluded that the rift started in the Miocene (~8.6 Ma) in the northern part of Malawi (Laó-Dávila et al., 2015). Van der Beek et al. (1998) estimated Oligocene ages (~30 Ma) from fission track of Precambrian apatite crystals in the northern rift (Laó-Dávila et al., 2015). However, radiometric dating in the RVC revealed ~18 Ma (Mesko et al., 2014; Grijalva et al., 2018) for the initiation in the northern part of the Malawi Rift.

3. Geological and structural setting

The oldest rocks in the North basin of the Malawi Rift are Precambrian grey gneisses (Fig. 1B and 2), and granite intrusions (e.g., Chapola & Kaphwiyo, 1992; Ray, 1975; Ring et al., 1999; Ring et al., 2002; Kolawole et al., 2018). The basement rocks present strong structural fabrics (Fig. 2 and 3A) with a general foliation oriented approx. $301^\circ/79^\circ$ NE (Dawson et al., 2018). In the western part of the Karonga basin, the Mesoproterozoic and Neoproterozoic Mughese Shear zone (MSZ) formed during a contractional episode between the Irumide and Ubendian Belts in the Neoproterozoic (Ring et al., 2002; Fritz et al., 2013; Dawson et al., 2018). The Ubendian Belt is a transcurrent NW-trending orogeny (Fig. 1B) where strike-slip deformation occurred repeatedly since the Paleoproterozoic (Delvaux, 2001; Fritz et al., 2013; Kolawole et al., 2018). The MSZ is the major subvertical shear belt in the north of Malawi (Fig. 1B) with a zone of 30 - 50 km wide and NW- trend (Ring et al., 2002).

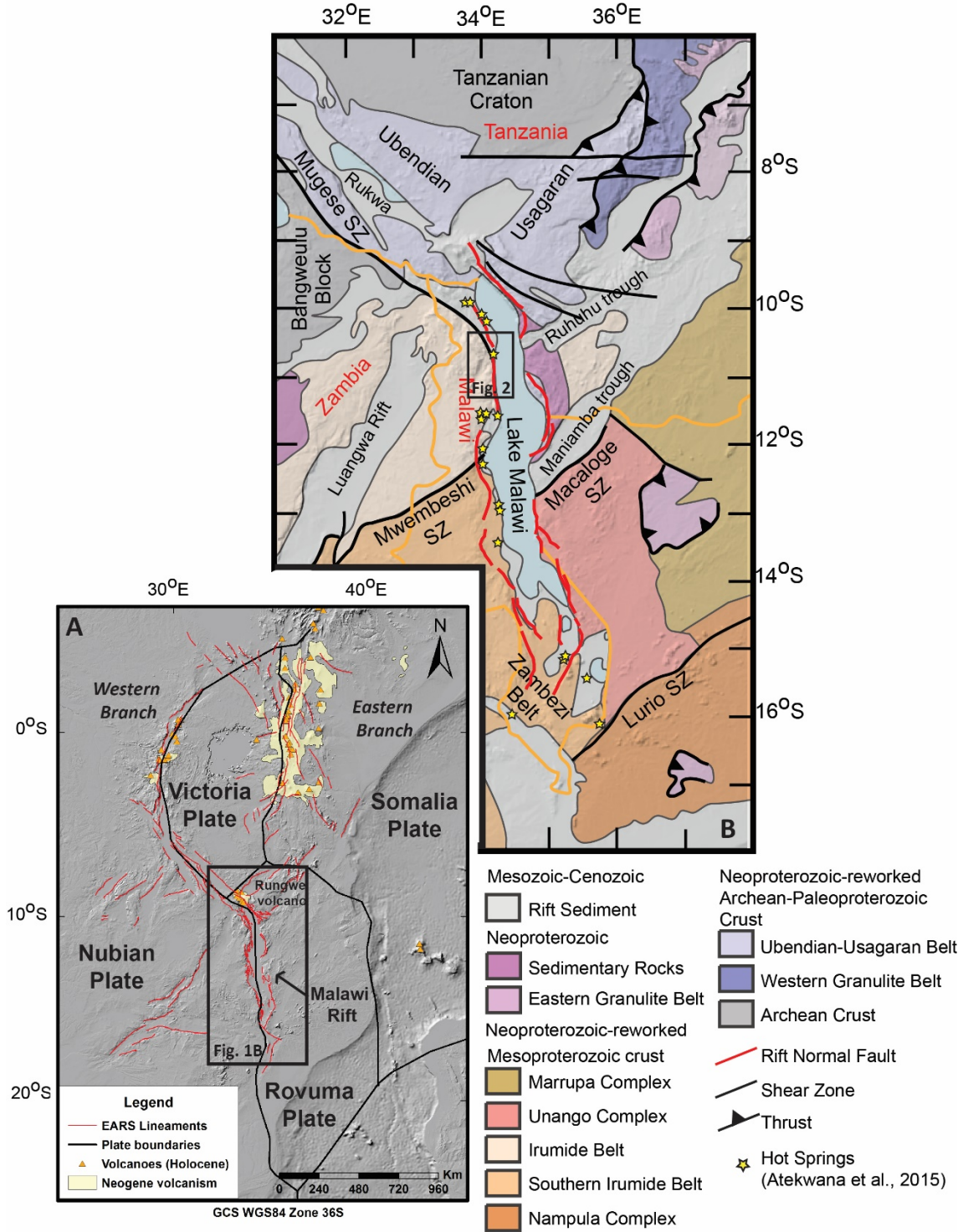


Fig. 1A. Global 30 arc second elevation data (GTOPO30) DEM showing the tectonic setting of the East African Rift System of the divergent boundary between Nubian and Somalia Plates and the Western and Eastern Branches of the rift. The Rungwe Volcanic complex is the only active volcano in the northern part of the Malawi Rift of Late Cenozoic age (Ebinger, 1989). **B.** Geological and structural map around the Malawi Rift. Modified after Laó-Dávila et al. (2015) and Fritz et al. (2013).

The Karoo rift basins were formed during the Late Carboniferous-Early Permian to Early Triassic times (Ring & Betzler, 1995; Delvaux, 2001), where sediments were deposited and consist roughly of conglomerates, sandstones, and coal measures (Chapola & Kaphwiyo, 1992). The Karoo basins consist of narrow and asymmetrical rifts bounded by major faults and exceed sediments accumulation of more than 3 km in thickness in some areas (Ring & Betzler, 1995). The NW-Trending Ubendian Belt in the north of Malawi associated with the MSZ was activated and filled with Karoo sediments during Late Carboniferous to Late Permian sediments (Fig. 2 and 3A). A major system of Karoo rift basins was developed along NE-trend (Delvaux, 2001). The most important NE-trend Karoo basin structures in the Malawi Rift are the Luangwa Rift, the Ruhuhu, Maniamba throughs, and the Shire Graben (Fig. 1B; Laó-Dávila et al., 2015).

Lacustrine sediments of the Quaternary are deposited onshore (Fig. 2) of the northwestern side of Lake Malawi (Chapola & Kaphwiyo, 1992). Moreover, in the northern part of Malawi Rift lie the RVC composed of basalt and nephelinite (Fig. 1A), which is the only volcano of the Malawi Rift of Late-Cenozoic age (Ebinger, 1989; Scholz et al., 2011).

The Malawi Rift has a ~N-S orientation and is suggested to be controlled by inherited structures (Fig. 1B and 3) associated with cratons, megashears, basement foliations, and pre-rift structures (Versfelt and Rosendahl, 1989; Ring, 1994; Lyons et al., 2011; Laó-Dávila et al., 2015). The structure of the Malawi Rift consists of seven asymmetric basins (Ebinger et al., 1989; Laó-Dávila et al., 2015; Kolawole et al., 2018). These seven asymmetric grabens are linked by accommodation and transfer zones (Flannery & Rosendahl, 1990; Ring & Betzler, 1995).

The Karonga Basin, Usisya Basin, Mbamba Basin, and the Bandwe Basin constitute the northern segment of the rift. This study is focused on the Karonga basin, where the Chiweta hot spring is located. The main fault system in the Karonga basin is the Livingstone fault (~120 km long) located in the eastern margin of Lake Malawi (Laó-Dávila et al., 2015) with a NW strike (Fig. 3A), more than 90 km of length, and > 10.4 km of dextral normal oblique-slip movement (Dawson et al., 2018; Wheeler & Karson, 1989).

The Karonga fault is 17.8 km long and lies to the western side of the rift and it is associated with the hanging wall of the Livingstone major fault (Fig. 3A), where the 2009 earthquakes occurred in the northwest region (Biggs et al., 2010; Laó-Dávila et al., 2015). In addition, Dawson et al. (2018) suggested that the Karonga fault was formed through the reactivated foliation planes of the Precambrian MSZ. The Karonga fault intersects the Ruhuhu Trough, and it is separated from the Usysia fault (Fig. 3A) by an ENE-trending accommodation zone (Specht and Rosendahl, 1989; Mortimer et al., 2007; Dawson et al., 2018). It is just in this intersection and accommodation zone where the Chiweta hot spring lies (Fig. 3B). The Usysia Fault is located in the western side of the north segment (Fig. 3B), and extends along ~200 km (Contreras et al., 2000; Laó-Dávila et al., 2015).

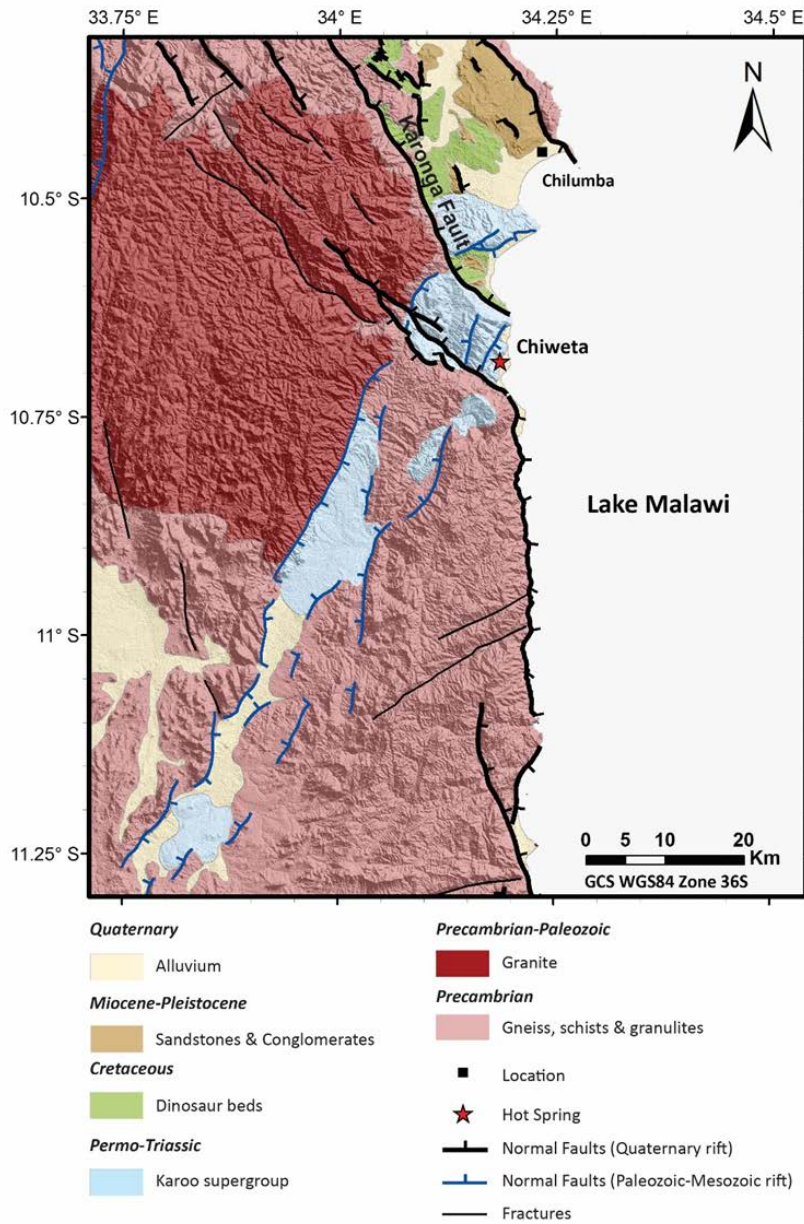


Fig. 2 Geological map of the northwest Malawi Rift southern from the Karonga area. The Chiweta hot spring lies in the Karoo succession near to the Chilumba locality. Modified from Geological Survey of Malawi (1966), Biggs et al. (2010), and Dawson et al. (2018).

4. Methods

4.1 Remote sensing analysis

A Shuttle Radar Topography Mission (SRTM) at 30 m spatial resolution was used to generate Digital Elevation Models (DEM) with the software ENVI 5.1. The generation of hill-shaded images, with a sun azimuth angles of 45° and an inclination of 45° , and the slope calculation method were used to highlight the major faults of the study area with different elevations. Subsequently, ArcMap was used to digitize different structures (faults, foliations, fractures, etc.) and Linear Directional Mean tool was used to calculate orientations (strikes) of the structures. Afterward, rose diagrams of the orientations were constructed using the software Stereonet v.10 (e.g. Allmendinger et al., 2012). These features allowed us to map the major shallow structural trends in the Chiweta geothermal zone. Our structural map was combined with previous maps of the Karonga area (Ring et al., 2002; Biggs et al., 2010; Laó-Dávila et al., 2015; Dawson et al., 2018). In addition, a topographic profile was extracted from the SRTM DEM to construct a geological cross-section of the Chiweta area.

4.2 Mohr circle diagram and Slip tendency

The Mohr circle diagram was constructed with MohrPlotter v.2.9 software by Allmendinger (2012). The Mohr circle is a representation of the normal and shear stress acting on a plane of different orientations through a point in the rock (Fossen, 2016; Allmendinger et al. 2012). We utilize three different normal faulting stress regimes measured to perform the Mohr circle diagrams:

- 1) Stress state proposed from focal mechanism stress inversion of the Malawi Rift by Delvaux and Barth (2010), where σ_3 is sub-horizontal ($06^\circ/242^\circ$), σ_2 is horizontal ($00^\circ/152^\circ$), and σ_1 is sub-vertical ($83^\circ/070^\circ$).
- 2) A second focal mechanism stress inversion of an earthquake in 2009 with Mb 5.9 at the north of Malawi compiled by the World Stress Map Project, where σ_3 is sub-horizontal ($10^\circ/073^\circ$), σ_2 is sub-horizontal ($07^\circ/342^\circ$), and σ_1 is very steep ($78^\circ/215^\circ$).
- 3) A third stress state performed from GPS measurements together with earthquakes slip vector directions by Saria et al. (2014), where σ_3 is horizontal ($00^\circ/086^\circ$), σ_2 is horizontal ($00^\circ/356^\circ$), and σ_1 is vertical ($90^\circ/300^\circ$).

A vertical stress gradient of 26.5 MPa/km was constrained taking into consideration an average density of 2.7 g/cm³ for the lithospheric crust (gneisses) following the equation:

$$P = \rho gz \tag{1}$$

where ρ is the density of the rock, g is acceleration due to gravity, and z is depth. The tensional stress of 8 MPa/km calculated by Coblenz and Sandiford (1994) from an elastic finite-element analysis in southern Africa was used in the Mohr circle diagram.

A stress ratio of $R \approx 0.50$ was taking in consideration following the results of Delvaux and Barth (2010). Stress ratio is defined as follow:

$$R = \sigma_2 - \sigma_3 / \sigma_1 - \sigma_3 \quad (2)$$

We performed the Mohr circle analysis for the main orientations (mean vector) resulted from the rose diagram analysis. We assumed various dips from 0 to 90° and performed the analysis at three different depths (1, 3, and 5 km). Then, failure was calculated increasing pore fluid pressure (P_f) for each depth. Afterward, the analysis was done for each orientation calculated from the Linear Directional Mean tool of the remote sensing analysis at 1 km depth (ideal geothermal target) assuming dips of 60° for faults and fractures, and dips of 90° for foliations (approx. dips measured in the field). Additionally, a coefficient of internal friction of 0.65 was chosen to take into consideration the rheology of gneiss rocks.

The fault segment to slip provides an indication of which sections of a fault zone within a geothermal system are most likely to transport geothermal fluids (Morris et al., 1996; Siler & Faulds, 2013). Morris et al. (1996) and Ferrill et al. (1999) defined slip tendency. Slip tendency (T_s) is defined by the ratio of shear stress (τ) to normal stress (σ_n) acting on that surface:

$$T_s = \tau / (\sigma_n - P_f) \quad (3)$$

where the normal stress is proportional to the frictional resistance to sliding (e.g. Jaeger and Cook, 1979) and P_f is pore fluid pressure. The MohrPlotter v.2.9 software can estimate failure by increasing P_f . We use this calculation to identify different values of P_f able to cause failure in pre-existing and new formed fractures. Slip will occur on a surface when the shear stress exceeds the frictional resistance to sliding (Morris et al., 1996). The failure envelopes utilize by the MohrPlotter v.2.9 software are the Griffith-Coulomb and frictional slip on pre-existing fractures. MohrPlotter v.2.9 software colors the planes, poles, and points on the Mohr diagram corresponding to their slip tendency (Morris and Ferrill, 2009). Hotter colors (red and orange) are more likely to slip than cooler colors (blue and green).

5. Results

5.1 Remote sensing analysis

The shallow expressions of the different structures presented in the Chiweta geothermal zone were traced as lineaments from the SRTM DEM image (Fig. 3). Subsequently, strikes were calculated and rose diagrams were generated in our study area. We identified four dominant structures presented in the Chiweta hot springs area (Fig. 3B): 1) Foliations associated with the MSZ with a general NW-SE-trend (Mean Vector= 129.9°). 2) Karoo faults of Paleozoic-Mesozoic age oriented NE-SW (Mean Vector= 026°). 3) Fractures with a general NW-SE-trend (Mean Vector= 130.4°). 4) Quaternary faults associated with the current rifting show a dominant trend NW-SE (Mean Vector= 324.3°) and a minor N-S orientation (Mean Vector= 355°) associated with the Usysia fault. 5) Additionally, intrabasin faults were digitalized from previous studies (Ring et al., 1995; Mortimer et al. 2007; Mortimer et al., 2016; and McCartney et al., 2016). The strikes of these structures are generally N-S (Mean Vector= 347.8°). Our results show three dominant structural orientations in the Chiweta geothermal zone NW-SE, NE-SW, and N-S trends (Fig. 3B).

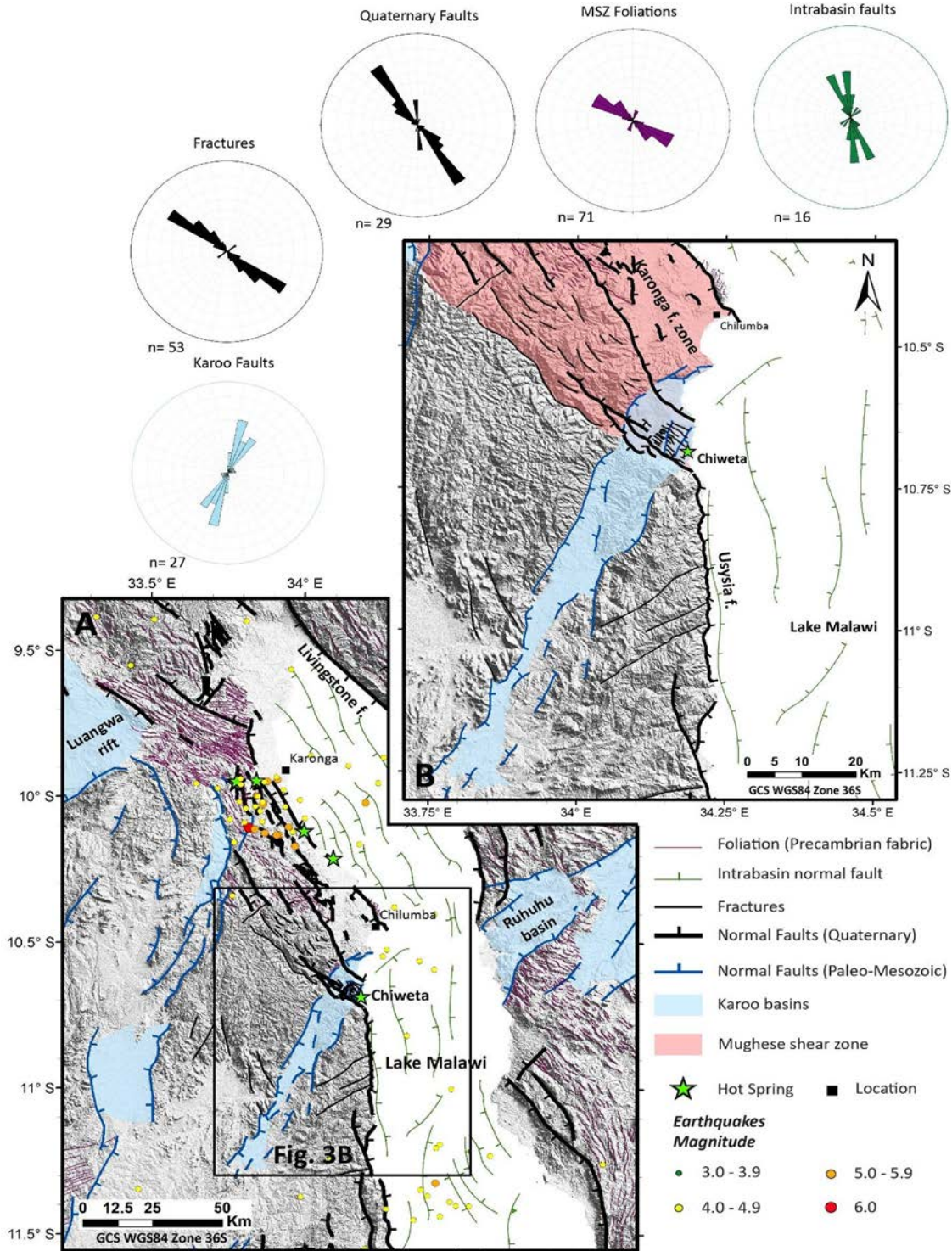


Fig. 3 A. Structural map of the northwest Malawi Rift generated from the Shuttle Radar Topography Mission (SRTM) Digital Elevation Model (DEM) modified from Laó-Dávila et al. (2015), and Dawson et al. (2018). The epicenters are from the United States Geological Survey (2019). The intrabasin faults modified from Ring et al. (1995); Mortimer et al. (2007); Mortimer et al. (2016), and McCartney et al. (2016). B. The structural map of the Chiweta zone showing the rose diagrams of major structures orientations. MSZ: Mughese Shear Zone.

5.2 Mohr circle diagram and Slip tendency

The results of the Mohr circle and slip tendency analysis of the mean vector and their orthogonal plane for three states of stress at different depths (1, 3, and 5 km) are summarized in Table 1. The results slightly vary depending on the stress state, but show the same results at different depths for each stress state. The pore fluid pressure (P_f) was estimated with the MohrPlotter v.2.9 software to cause failure and create new-formed fractures. In general, the pore fluid pressure tends to increase at depth (Table 1).

The results show that for the pre-existing fractures with a cohesion equal to zero the structures oriented ~NW-SE and ~N-S tend to have high slip tendency (Fig. 4A-B) for the two first states of stress ($\sigma_3=06^\circ/242^\circ$ and $\sigma_3=10^\circ/073^\circ$). The dips with high slip tendency diverge for each state stress but at least all have high slip tendency at dips of 60° , as Anderson's theory of normal faulting indicates (Table 1). The dips ranges of pre-existing fractures with high slip tendency increase considerably when pore fluid pressure is calculated to cause failure in rocks with cohesion equal to 11 MPa and ~NE-SW structures could undergo slip for the last two states of stress in these conditions (Table 1, Fig. 4C-D).

Table 1. Summary of the Mohr circle diagram and slip tendency results done for three states of normal stress and the mean vector orientations and their orthogonal planes.

Stress State	High Slip Tendency				
	Pre-existing Fractures $P_f = 0$ (Strike/Dip)	Pre-existing Fractures $P_f \neq 0$ (Strike/Dip)	Failure New Fractures		
			1 km	3 km	5 km
$\sigma_3=06/242$	~130/60-70 – 310/ 40-60 ~144/50-80 – 324/40-60 ~167/50-80 – 347/40-60 ~175/60-80 – 355/40-60	~130/50-90 – 310/ 30-90 ~144/50-90 – 324/30-70 ~167/50-90 – 347/30-70 ~175/50-90 – 355/30-90	$P_f=3.67$	$P_f=11.05$	$P_f=18.44$
			332/56	332/56	332/56
$\sigma_3=10/073$	~130/50 – 310/ 70-80 ~144/40-60 – 324/60-80 ~167/40-60 – 347/60-80 ~175/40-60 – 355/60-80	~130/30-90 – 310/ 50-90 ~144/20-90 – 324/50-90 ~167/20-90 – 347/40-90 ~175/20-90 – 355/40-90 ~026/50-90 – 206/30-90	$P_f=6.83$	$P_f=20.6$	$P_f=32.13$
			167/53	167/53	167/52
$\sigma_3=00/086$	~144/40-60 – 324/60-80 ~167/50-70 – 347/50-70 ~175/50-70 – 355/50-70 ~026/60-70 – 206/60-70	~130/40-90 – 310/ 40-90 ~144/40-90 – 324/40-90 ~167/30-90 – 347/30-90 ~175/30-90 – 355/30-80 ~026/40-90 – 206/40-90	$P_f=7$	$P_f=20.9$	$P_f=22.7$

The orientations of the planes are the mean vector and their orthogonal calculated with the rose diagram (Fig. 3) for each of the different structures (faults, fractures, and foliations) in the study area. P_f is pore fluid pressure.

The slip tendency analysis performed by each of the main structures at 1 km depth with dips of 60° for faults and fractures, and 90° for foliations are summarized in Fig. 5. The Quaternary faults with structures ~NW-SE and ~N-S show a higher slip tendency in the two first states of stress (Fig. 5 A-B). Whereas, the third state stress shows faults oriented ~N-S with high slip tendency (Fig. 5C). The intrabasin faults show high slip tendency in ~N-S directions for all states of stress (Fig. 5D-E). The Karoo faults oriented ~NNE-SSW show higher slip tendency for the last state stress (Fig. 5I). The fractures oriented ~NW-SE have higher slip tendency in the two first states of stress (Fig. J-K). The foliations ~NW-SE and ~N-S dipping 90° do not display high slip tendency (Fig. 5M-O). The pore fluid pressure should be higher than 4 MPa in order to slip a foliation plane with dips of 90° (Fig. 6C-D). The first state stress has a preferential failure plane oriented ~332°/56°, the second is oriented ~167°/53°, and the last state stress presents a failure plane oriented ~176°/63° (Table 1).

6. Discussions

6.1 Geothermal overview

The Chiweta hot spring is the highest geothermal manifestation in the Malawi Rift with a temperature of ~75° C on the surface, and a reservoir temperature of ~ 200°C estimated with Na-K geothermometers (Dávalos-Elizondo et al., 2018). The chemistry of the waters and the stable isotopic signature of the Chiweta hot spring is slightly distinct from the rest of the hot springs in Malawi. Chiweta shows higher chloride concentrations and an increment of δD and mainly $\delta^{18}O$ isotopes, which makes it of great interest for a geothermal exploration perspective. Previous studies suggested the presence of high heat flow between 77 to 120 mW/m² in the continental crust (Von Herzen & Vacquier, 1967; Njinju et al., 2015) beneath the Malawi Rift. The source of this high heat flow is not really understood; the only Cenozoic volcanic activity presented is the Rungwe volcanic complex in the most northern part of the rift.

Recently, Grijalva et al. (2018) and Wang et al (2019) carried out a seismic tomography model in the northern and southern part of the Malawi Rift, respectively. Grijalva et al. (2018) showed a low-velocity zone (P-S waves) at depths around 50 - 150 km that extends beneath the Bangweulu craton and the RVC in the northern Malawi. They interpreted the anomaly as a super mantle plume and suggested that volcanic activity of about 10 Ma in the RVC is assisting rifting and weakening the lithosphere underlying the northern of the rift. Other authors suggested a high heat flow associated with isotopic decay of Uranium deposits from the Karoo sediments of Paleo-Mesozoic age (e.g. Njinju, 2012). However, Wang et al. (2019) mentioned that temperatures calculated from heat flow values (about 77 mW/m²; Njinju et al., 2015) alone are not enough to produce the low velocities beneath the southern part of the rift. Although no surface volcanic activity is occurring southward of the rift, this does not dismiss the possibility of a magmatic intrusion at depth may be presented in this region (Fagereng, 2013). Regardless the source of heat in the Malawi Rift several studies have been concluded that the geothermal systems in the Malawi rift are strongly fault controlled, where meteoric waters are infiltrated and heated by a moderate geothermal gradient by deep circulation along the faults (e.g., Atekwana et al., 2015; Dávalos-Elizondo et al., 2018).

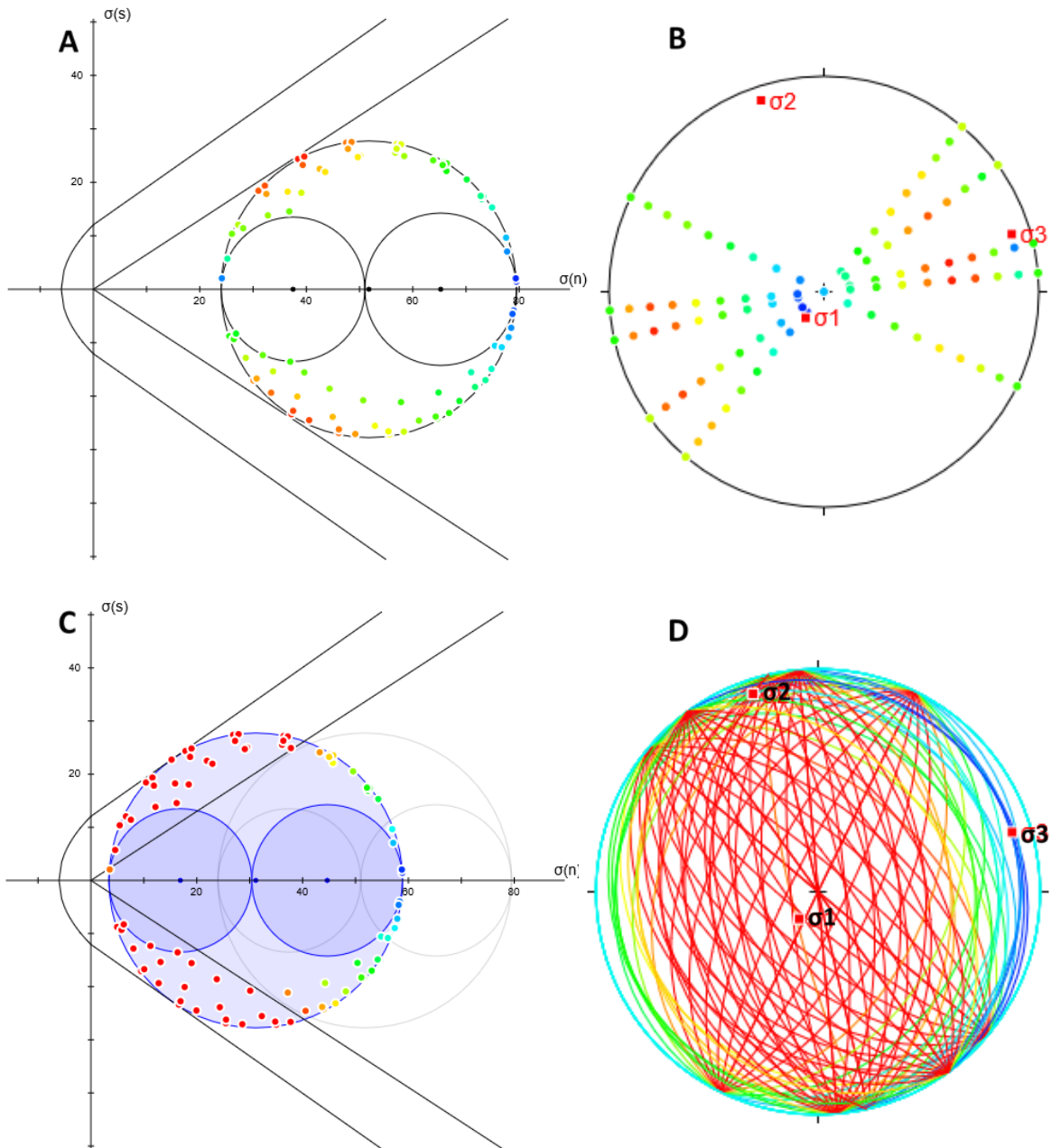


Fig. 4. Stress State where σ_3 is oriented 10/073 performed at 3 km. **A.** Mohr circle diagram and slip tendency analysis showing the mean vector orientations of the main structural planes in the study area without pore fluid pressure **B.** Stereonet showing the principal compressional stresses and the poles of the planes. **C.** Mohr circle diagram and slip tendency analysis showing the calculation of failure within increasing the fluid pure pressure ($P_f = 20.6$ MPa). **D.** Stereonet showing the principal compressional stresses and the great circles of the planes with failure calculation ($P_f = 20.6$ MPa). Red and orange indicate higher slip tendency than blue and green. Coefficient of internal friction= 0.65. Cohesion= 0 in preexisting fractures of a critical state of stress envelope, and cohesion= 11 MPa and tensile strength= - 5.5 MPa of rocks without fractures of a stable envelope.

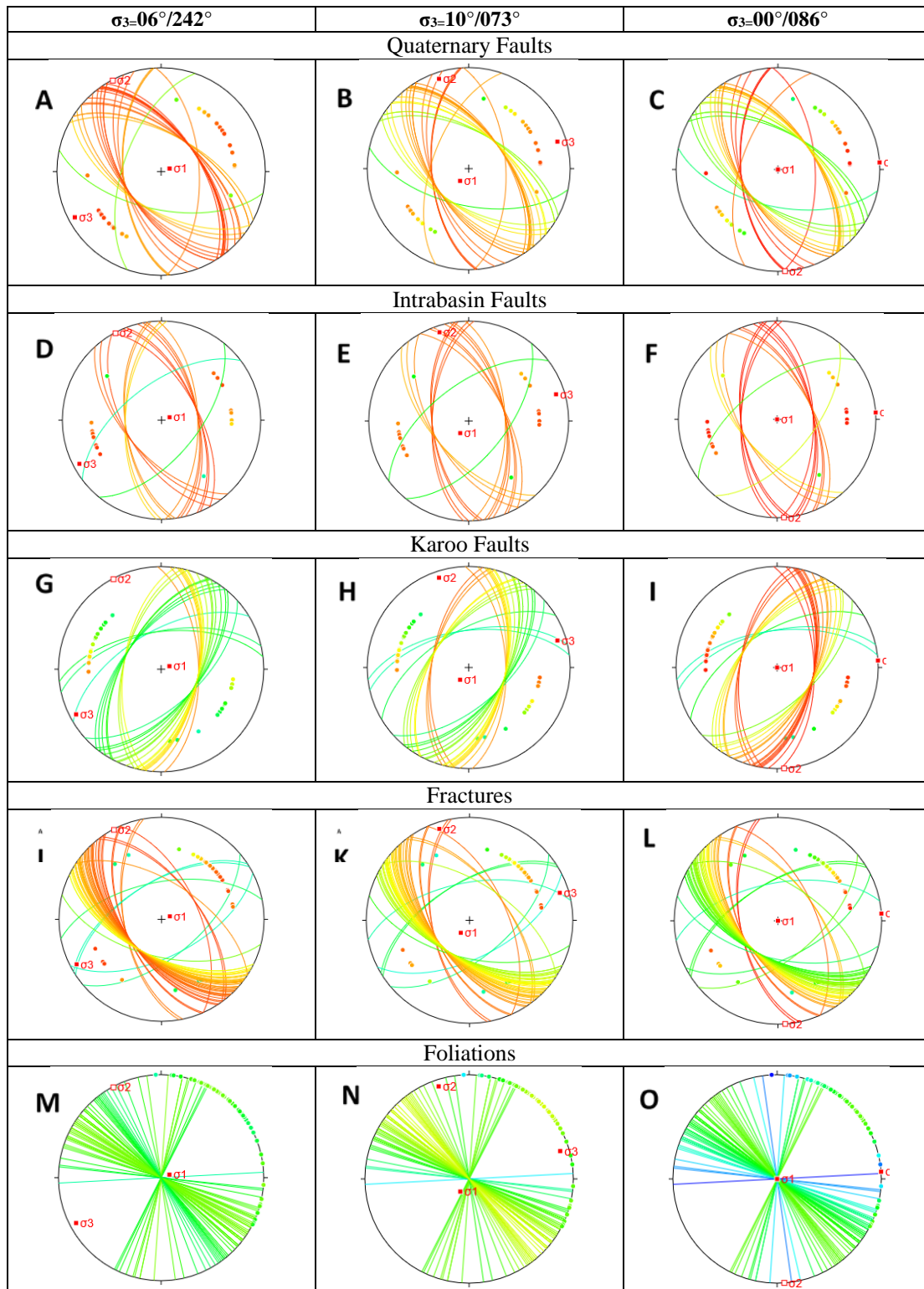


Fig. 5. Slip tendency analysis of the three states of stress showing stereonets of the main structures (great circles and poles). Hotter colors are high slip tendency and cooler colors low slip tendency.

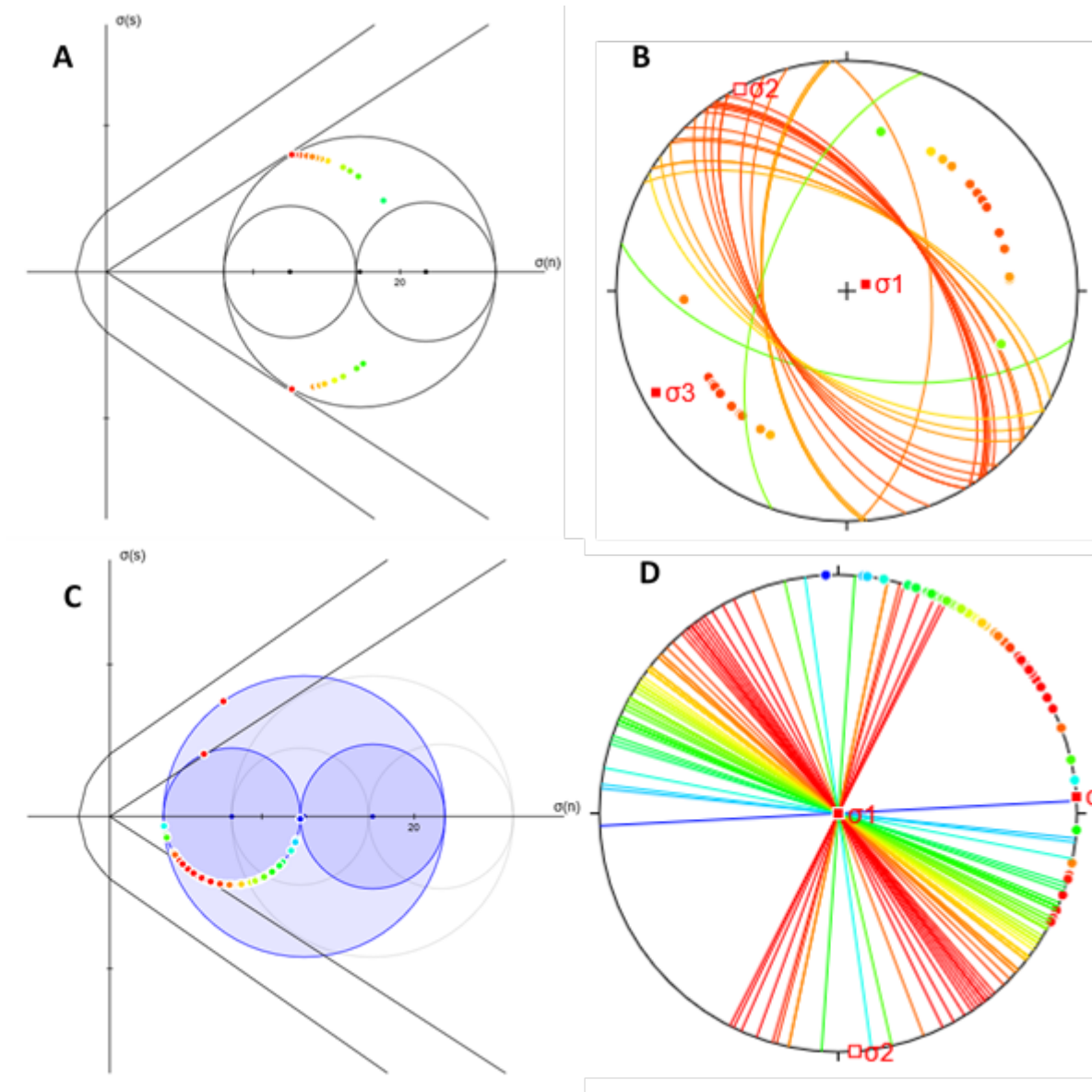


Fig. 6. A. Mohr circle analysis and slip tendency where σ_3 is oriented $06^\circ/242^\circ$ performed at 1 km without pore fluid pressure (Quaternary faults). B. Stereonet showing the principal compressional stresses and the poles of the Quaternary faults. C. Mohr circle diagram and slip tendency analysis where σ_3 is oriented $00^\circ/086^\circ$ showing the calculation of failure within increasing the pore fluid pressure ($P_f = 3.97$ MPa). D. Stereonet showing the principal compressional stresses and the great circles of the planes with failure calculation ($P_f = 3.97$ MPa). Red and orange indicate higher slip tendency than blue and green. Coefficient of internal friction = 0.65. Cohesion = 0 in preexisting fractures of a critical state of stress envelope, and cohesion = 11 MPa and tensile strength = -5.5 MPa. of rocks without fractures of a stable envelope.

6.2 Favorable structures and permeable zones

There are several studies focused on understanding the role of favorable structures in the transportation and storage of geothermal fluids (e.g., Barton et al., 1995; Evans et al., 1997; Blackwell et al., 1999; Faulds et al., 2006; Faulds et al., 2011; Siler and Faulds., 2013). The identification of these structural controls in a particular region, such as the Basin and Range in United States, has contributed to identifying several hidden or blind geothermal systems in this region, where little or no surface manifestation is evident and volcanic activity is not present (e.g. Faulds et al., 2011; Siler and Faulds, 2013; Faulds et al., 2013).

The Malawi Rift is characterized by asymmetric basins flanked by major faults (Fig. 7), usually with alternating polarity (e.g., Rosendahl et al., 1992). It is right in this segmentation or alternating polarity between the major Livingstone fault (NW-SE) and the Usysia fault (N-S) where the Chiweta hot spring is located (Fig. 3 and 7). These accommodation zones are favorable structural controls of geothermal fluids reported by other studies (e.g., Faulds and Varga, 1998; Faulds et al., 2011). Faulds and Varga (1998) defined a transfer zone as a discrete zone of strike-slip and oblique-slip faulting parallel to the extension direction that typically arranged an echelon pattern. Whereas, accommodation zones as belts of overlapping fault terminations divided by dipping normal faults or adjacent domains of oppositely dipping normal fault. They can be parallel, perpendicular, or oblique to the extensional direction (Faulds and Varga, 1998).

Our remote sensing analysis suggested that the Chiweta hot spring is located in an accommodation zone where the Livingstone fault oriented ~NW-SE is changing polarity abruptly to ~N-S orientation of the Usysia fault (Fig. 3 and 7), approximately ~50 km across Lake Malawi. Locally, the Chiweta hot spring lies right in the termination of the Mughese shear zone, Quaternary rift faults (~NW-SE), and the Usysia fault (~N-S). Additionally, the Quaternary rift (Lake Malawi) bisects the Karoo basin (~NE-SW faults) right in the location of the Chiweta hot spring. We suggest that the Chiweta hot spring lies in a synthetic zone of the hinge zone where a relay ramp connects the hanging wall of a fault to the footwall of another fault. Additionally, the Usysia fault termination and the bisected Karoo faults are intersecting this area (Fig. 7), improving the permeability. The remote sensing analysis in this study shows these three dominant structural orientations (NW-SE, NE-SW, and N-S) in the Chiweta geothermal zone (Fig. 3B). This intersection of major structures with different strikes is a favorable permeable zone for controlling geothermal fluids

The Mohr circle and slip tendency analysis show a high slip tendency for structures mainly oriented ~NW-SE and ~N-S and dipping ~60°. These structures could be the main pathways of the hot fluids to the surface in the Chiweta geothermal zone. Whereas, the NE-SW structures associated with the Karoo basins, with moderate slip tendency are possible confining structures of the geothermal system. On the other hand, the foliation structures with dips around 90° that

show low to medium slip tendency could be reactivated when fluid pore pressure is high in presence of fluids, as the Chiweta geothermal zone.

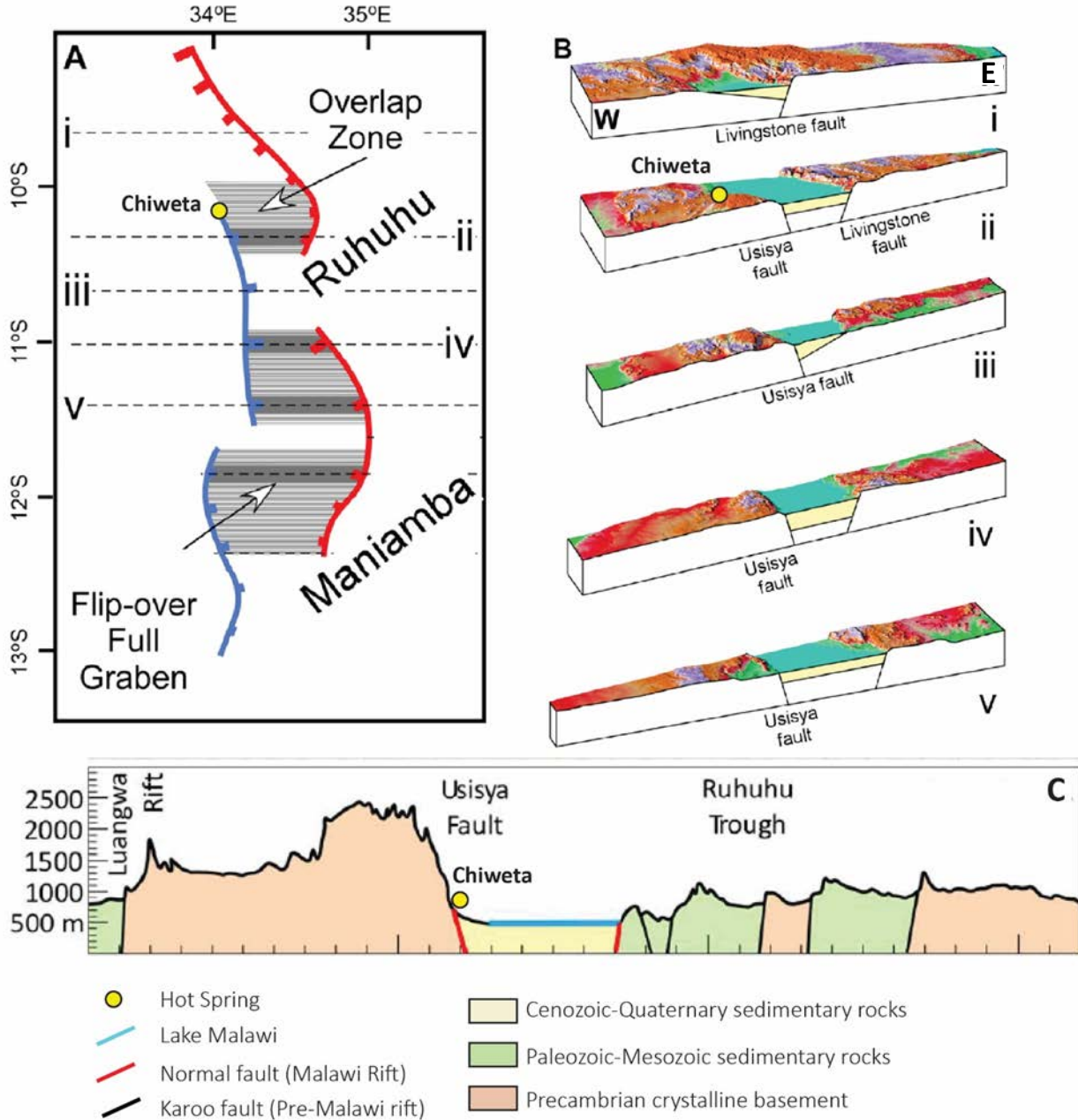


Fig. 7. A. Malawi rift idealized model of the northern area showing the location of the Chiweta hot spring in the accommodation zone and the half-graben polarity alternation east to west dipping. B. 3D topographic cross-sections of different slices of the northern part of the rift and the location of the Chiweta hot spring. C. East-West trending geological section ii across the Malawi Rift (Fig. 7A) showing the projection of the Chiweta hot spring. The topographic profile is extracted from the Shuttle Radar Topography Mission (SRTM)-DEM with vertical exaggeration of 2.0. Modified from Laó-Dávila et al. (2015).

7. Conclusions

The Chiweta geothermal zone is associated with moderate heat flow and a geothermal fault control system. The favorable structure that controls the transporting and storage of the Chiweta geothermal system is associated with the Livingstone-Usysia accommodation zone, where relay ramps linking the hanging wall of faults to the footwall of other faults. This accommodation zone is located in the hinge zone of the major Livingstone fault, where Quaternary faults (~NW-SE) and inherited structures of the Mughese shear zone (~NW-SE) dominate the relief. Furthermore, the Chiweta hot springs lie right where Quaternary faults bisect the Karoo faults (~NE-SW faults). All these intersections and overlapping structures are assisting permeability in this area. Moreover, the remote sensing analysis support that structures ~NW-SE, NE-SW and N-S are predominant in the Chiweta zone. The ~NW-SE and ~N-S pre-existing structures of Quaternary ages with ~60° dip have high slip tendency and are possibly the main pathways of the geothermal fluids. Whereas the ~NE-SW pre-existing structures of Paleo-Mesozoic age have moderate slip tendency in the presence of the local stress state and could be confining structures of the geothermal system. Moreover, the pore fluid pressures increase the slipping tendency and it is probably higher in areas where fluids are present, as the Chiweta hot spring. The future of this study will focus on aeromagnetic data, slip and dilation tendency analysis, and three-dimensional fault geometry in order to identify the most permeable zones in the north part of the rift.

Acknowledgement

We are grateful to all the anonymous reviewers and editors whose thorough, critical, helpful, constructive comments helped to improve this manuscript. The authors are especially grateful to Steven Johnson for all his support and help during the elaboration of this manuscript. We are grateful to the Boone Pickens School of Geology and the Tectonics Group for all the support during this research. Estefanny Dávalos-Elizondo is supported by a Dawson Geophysical scholarship and Gary F. Stewart Scholarship. This research was awarded with the Geothermal Resources Council Scholarship 2018.

REFERENCES

- Allmendinger, RW. "Stereonet 7.2. 4." 2012.
- Atekwana, E., Tsokonombwe, G., Elsenbeck, J., Wanless, V., and Atekwana, E. "Chemical and Isotopic Characteristics of Hot Springs along the Neogene Malawi Rift." *Paper presented at the AGU Fall Meeting Abstracts*, (2015).
- Barton, C. A., Zoback, M. D., and Moos, D. "Fluid Flow along Potentially Active Faults in Crystalline Rock." *Geology* 23, no. 8 (1995): 683-86.
- Biggs, J., Nissen, E., Craig, T., Jackson, J., and Robinson, D. P. "Breaking up the Hanging Wall of a Rift-Border Fault: The 2009 Karonga Earthquakes, Malawi." *Geophysical Research Letters* 37, no. 11 (2010).

- Blackwell, D., Wisian, K. W., Benoit, D., and Gollan, B. "Structure of the Dixie Valley Geothermal System, a " Typical" Basin and Range Geothermal System, from Thermal and Gravity Data." *Transactions-Geothermal Resources Council* (1999): 525-32.
- Bloomfield, K. "The Geology of the Zomba Area." *Government Printer*, South Africa, (1965).
- Bloomfield, K., and Garson, M.S. "The Geology of the Kirk Range, Lisungwe Valley Area." *Government Printer*, (1965).
- Calais, E., d'Oreye, N., Albaric, J., Deschamps, A., Delvaux, D., Deverchere, J., Ebinger, C., Ferdinand, R. W., Kervyn, F., Macheyeke, A. S., Oyen, A., Perrot, J., Saria, E., Smets, B., Stamps, D. S., and Wauthier, C. "Strain Accommodation by Slow Slip and Dyking in a Youthful Continental Rift, East Africa." *Nature* 456, no. 7223 (Dec 11 2008): 783-7.
- Chapola, L.S., and Kaphwiyo, C.E. "The Malawi Rift: Geology, Tectonics and Seismicity." *Tectonophysics* 209, no. 1-4 (1992): 159-64.
- Chorowicz, J. "The East African Rift System." *Journal of African Earth Sciences* 43, no. 1-3 (2005): 379-410.
- Coblentz, D., and Sandiford, M. "Tectonic Stresses in the African Plate: Constraints on the Ambient Lithospheric Stress State." *Geology* 22, no. 9 (1994): 831-34.
- Contreras, J., Anders, M. H., and Scholz, C. H. "Growth of a Normal Fault System: Observations from the Lake Malawi Basin of the East African Rift." *Journal of Structural Geology* 22, no. 2 (2000): 159-68.
- Corti, G., van Wijk, J., Cloetingh, S., and Morley, C. K. "Tectonic Inheritance and Continental Rift Architecture: Numerical and Analogue Models of the East African Rift System." *Tectonics* 26, no. 6 (2007).
- Dávalos-Elizondo, E., Atekwana, E.A., Atekwana, E. A., Tsokonombwe, G., and Laó-Dávila, D.A. "Geothermometry of Hot Springs in the Malawi Rift". *Poster presented at the GSA Annual Meeting*, (2018).
- Dawson, S. M., Laó-Dávila, D. A., Atekwana, E. A., and Abdelsalam, M. G. "The Influence of the Precambrian Mughese Shear Zone Structures on Strain Accommodation in the Northern Malawi Rift." *Tectonophysics* 722 (2018): 53-68.
- Delvaux, D. "Karoo Rifting in Western Tanzania: Precursor of Gondwana Breakup." *Contributions to geology and paleontology of Gondwana in honor of Helmut Wopfner*: Cologne, Geological Institute, University of Cologne (2001): 111-25.
- Delvaux, D., and Barth, A. "African Stress Pattern from Formal Inversion of Focal Mechanism Data." *Tectonophysics* 482, no. 1-4 (2010): 105-28.
- Dixey, F. "The Tertiary and Post-Tertiary Lacustrine Sediments of the Nyasan Rift-Valley." *Quarterly Journal of the Geological Society* 83, no. 1-5 (1927): 432-42.
- Dulanya, Z. "Geothermal Resources of Malawi—an Overview." *Paper presented at the Thirty-First Workshop on Geothermal Reservoir Engineering*, (2006).
- Dulanya, Z., Morales-Simfors, N., and Sivertun, Å. "Comparative Study of the Silica and Cation Geothermometry of the Malawi Hot Springs: Potential Alternative Energy Source." *Journal of African Earth Sciences* 57, no. 4 (2010): 321-27.

- Ebinger, C. J. "Tectonic Development of the Western Branch of the East African Rift System." *Geological Society of America Bulletin* 101, no. 7 (1989): 885-903.
- Ebinger, C. J., Deino, A. L., Tesha, A. L., Becker, T., and Ring, U. "Tectonic Controls on Rift Basin Morphology: Evolution of the Northern Malawi (Nyasa) Rift." *Journal of Geophysical Research: Solid Earth* 98, no. B10 (1993): 17821-36.
- Ebinger, C.J., and Casey, M. "Continental Breakup in Magmatic Provinces: An Ethiopian Example." *Geology* 29, no. 6 (2001): 527-30.
- Evans, J. P., Forster, C. B., and Goddard, J. V. "Permeability of Fault-Related Rocks, and Implications for Hydraulic Structure of Fault Zones." *Journal of structural Geology* 19, no. 11 (1997): 1393-404.
- Fagereng, Å. "Fault Segmentation, Deep Rift Earthquakes and Crustal Rheology: Insights from the 2009 Karonga Sequence and Seismicity in the Rukwa–Malawi Rift Zone." *Tectonophysics* 601 (2013): 216-25.
- Faulds, J. E., and Varga, R. J. "The Role of Accommodation Zones and Transfer Zones in the Regional Segmentation of Extended Terranes." *Geological Society of America Special Papers* 323 (1998): 1-45.
- Faulds, J. E., Coolbaugh, M. F., Vice, G. S., and Edwards, M. L. "Characterizing Structural Controls of Geothermal Fields in the Northwestern Great Basin: A Progress Report." *Geothermal Resources Council Transactions* 30 (2006): 69-76.
- Faulds, J. E., Hinz, N. H., Coolbaugh, M. F., Cashman, P. H., Kratt, C., Dering, G., Edwards, J., Mayhew, B., and McLachlan, H. "Assessment of Favorable Structural Settings of Geothermal Systems in the Great Basin, Western USA." *Geothermal Resources Council Transactions* 35 (2011): 777-83.
- Faulds, James E, Nicholas H Hinz, Gregory M Dering, and Drew L Siler. "The Hybrid Model—the Most Accommodating Structural Setting for Geothermal Power Generation in the Great Basin, Western USA." *Geothermal Resources Council Transactions* 37 (2013): 3-10.
- Ferrill, D. A., Winterle, J., Wittmeyer, G., Sims, D., Colton, S., Armstrong, A., and Morris, A. P. "Stressed Rock Strains Groundwater at Yucca Mountain, Nevada." *GSA Today* 9, no. 5 (1999): 1-8.
- Flannery, J., and Rosendahl, B. "The Seismic Stratigraphy of Lake Malawi, Africa: Implications for Interpreting Geological Processes in Lacustrine Rifts." *Journal of African Earth Sciences (and the Middle East)* 10, no. 3 (1990): 519-48.
- Fossen, H. "Structural Geology". *Cambridge University Press*, 2016.
- Fritz, H., Abdelsalam, M., Ali, K. A., Bingen, B., Collins, A. S., Fowler, A. R., Ghebreab, W., Hauzenberger, C. A., Johnson, P. R., Kusky, T. M., Macey, P., Muhongo, S., Stern, R. J., and Viola, G. "Orogen Styles in the East African Orogen: A Review of the Neoproterozoic to Cambrian Tectonic Evolution." *J Afr Earth Sci* 86 (Oct 2013): 65-106.
- Fritz, H., Abdelsalam, M., Ali, K. A., Bingen, B., Collins, A. S., Fowler, A. R., Ghebreab, W., Hauzenberger, C. A., Johnson, P. R., Kusky, T. M., Macey, P., Muhongo, S., Stern, R. J., and Viola, G. "Orogen Styles in the East African Orogen: A Review of the Neoproterozoic to Cambrian Tectonic Evolution." *J Afr Earth Sci* 86 (Oct 2013): 65-106.

- Goldsworthy, M., and Jackson, J. "Migration of Activity within Normal Fault Systems: Examples from the Quaternary of Mainland Greece." *Journal of Structural Geology* 23, no. 2-3 (2001): 489-506.
- Gondwe, K., Allen, A., Georgsson, L., Loga, U., and Tsokonombwe, G., "Geothermal Development in Malawi—a Country Update", in *Proceedings 4th African Rift Geothermal Conference*, Nairobi, Kenya 2015, p. 21-23.
- Grijalva, A., Nyblade, A. A., Homman, K., Accardo, N. J., Gaherty, J. B., Ebinger, C. J., Shillington, D. J., Chindandali, P. R., Mbogoni, G., and Ferdinand, R. W. "Seismic Evidence for Plume and Craton Influenced Upper Mantle Structure beneath the Northern Malawi Rift and the Rungwe Volcanic Province, East Africa." *Geochemistry, Geophysics, Geosystems* (2018).
- Harrison, D.R., and Chapusa, F.W.P. "The Geology of the Nkhotakota-Benga Area." *Government Printer*, (1975).
- Heidbach, O., Fuchs, K., Muller, B., Wenzel, F., Reinecker, J., Tingay, M., and Sperner, B. "The World Stress Map." (2007).
- Kalebe, Y.N. "Chemical and Isotopic Composition of Thermal Waters in Northern Part of Malawi." (2018).
- Klerkx, J., Theunissen, K., and Delvaux, D. "Persistent Fault Controlled Basin Formation since the Proterozoic along the Western Branch of the East African Rift." *Journal of African Earth Sciences* 26, no. 3 (1998): 347-61.
- Kolawole, F., Atekwana, E. A., Laó Dávila, D. A., Abdelsalam, M. G., Chindandali, P. R., Salima, J., and Kalindekafe, L. "Active Deformation of Malawi Rift's North Basin Hinge Zone Modulated by Reactivation of Preexisting Precambrian Shear Zone Fabric." *Tectonics* 37, no. 3 (2018): 683-704.
- Laó-Dávila, D. A., Al-Salmi, H. S., Abdelsalam, M. G., and Atekwana, E. A. "Hierarchical Segmentation of the Malawi Rift: The Influence of Inherited Lithospheric Heterogeneity and Kinematics in the Evolution of Continental Rifts." *Tectonics* 34, no. 12 (2015): 2399-417.
- Lyons, R. P., Scholz, C. A., Buoniconti, M. R., and Martin, M. R. "Late Quaternary Stratigraphic Analysis of the Lake Malawi Rift, East Africa: An Integration of Drill-Core and Seismic-Reflection Data." *Palaeogeography, Palaeoclimatology, Palaeoecology* 303, no. 1-4 (2011): 20-37.
- McCartney, T., and Scholz, C. A. "A 1.3 Million Year Record of Synchronous Faulting in the Hangingwall and Border Fault of a Half-Graben in the Malawi (Nyasa) Rift." *Journal of Structural Geology* 91 (2016): 114-29.
- McConnell, R.B. "Geological Development of the Rift System of Eastern Africa." *Geological Society of America Bulletin* 83, no. 9 (1972): 2549-72.
- Mesko, G., Class, C., Maqway, M., Boniface, N., Manya, S., and Hemming, S. "Migration of Activity within Normal Fault Systems: Examples from the Quaternary of Mainland Greece." *Journal of Structural Geology* 23, no. 2-3 (2001): 489-506.
- Morris, A. P., and Ferrill, D. A. "The Importance of the Effective Intermediate Principal Stress ($\Sigma' 2$) to Fault Slip Patterns." *Journal of Structural Geology* 31, no. 9 (2009): 950-59.

- Morris, A., Ferrill, D. A., and Henderson, D. B. "Slip-Tendency Analysis and Fault Reactivation." *Geology* 24, no. 3 (1996): 275-78.
- Mortimer, E., Kirstein, L. A., Stuart, F. M., and Strecker, M. R. "Spatio-Temporal Trends in Normal-Fault Segmentation Recorded by Low-Temperature Thermochronology: Livingstone Fault Scarp, Malawi Rift, East African Rift System." *Earth and Planetary Science Letters* 455 (2016): 62-72.
- Mortimer, E., Paton, D. A., Scholz, C. A., Strecker, M. R., and Blisniuk, P. "Orthogonal to Oblique Rifting: Effect of Rift Basin Orientation in the Evolution of the North Basin, Malawi Rift, East Africa." *Basin Research* 19, no. 3 (2007): 393-407.
- Msika, B. J., Saka, J. D. K., & Dulanya, Z. "Spatial Distribution, Chemistry and Subsurface Temperatures of Geothermal Springs Nkhata Bay, Malawi." *African Journal of Environmental Science and Technology* 8, no. 8 (2014): 464-75.
- Njinju, E. A., Atekwana, E. A., Mickus, K. L., Laó-Dávila, D. A., Abdelsalam, M. G., and Atekwana, E. A., "Geophysical Investigation of Thermal Structures beneath the Malawi Rift." In Seg Technical Program Expanded Abstracts 2015, 1578-83: *Society of Exploration Geophysicists*, 2015.
- Njinju, E.A. "Crustal and Sub-Continental Lithospheric Mantle Decoupling beneath the Malawi Rift." *Unpublished Master's Thesis, Oklahoma State University, Stillwater, OK* (2012).
- Ray, G.E. "The Geology of the Chitipa-Karonga Area". *Government Printer, South Africa*, 1975.
- Ring, U. "Aspects of the Kinematic History and Mechanisms of Superposition of the Proterozoic Mobile Belts of Eastern Central Africa (Northern Malawi and Southern Tanzania)." *Precambrian Research* 62, no. 3 (1993): 207-26.
- Ring, U. "The Influence of Preexisting Structure on the Evolution of the Cenozoic Malawi Rift (East African Rift System)." *Tectonics* 13, no. 2 (1994): 313-26.
- Ring, U., and Betzler, C. "Geology of the Malawi Rift: Kinematic and Tectonosedimentary Background to the Chiwondo Beds, Northern Malawi." *Journal of Human Evolution* 28, no. 1 (1995): 7-21.
- Ring, U., Kröner, A., Buchwaldt, R., Toulkeridis, T., and Layer, P. W. "Shear-Zone Patterns and Eclogite-Facies Metamorphism in the Mozambique Belt of Northern Malawi, East-Central Africa: Implications for the Assembly of Gondwana." *Precambrian Research* 116, no. 1-2 (2002): 19-56.
- Ring, U., Kröner, A., Layer, P., Buchwaldt, R., and Toulkeridis, T. "Deformed a-Type Granites in Northern Malawi, East-Central Africa: Pre-or Syntectonic?" *Journal of the Geological Society* 156, no. 4 (1999): 695-714.
- Roberts, E. M., Stevens, N. J., O'Connor, P. M., Dirks, P. H. G. M., Gottfried, M. D., Clyde, W. C., Armstrong, R. A., Kemp, A. I. S., and Hemming, S. "Initiation of the Western Branch of the East African Rift Coeval with the Eastern Branch." *Nature Geoscience* 5, no. 4 (2012): 289-94.

- Rosendahl, B. R., Kilembe, E., and Kaczmarick, K. "Comparison of the Tanganyika, Malawi, Rukwa and Turkana Rift Zones from Analyses of Seismic Reflection Data." *Tectonophysics* 213, no. 1-2 (1992): 235-56.
- Saria, E., Calais, E., Stamps, D., Delvaux, D., and Hartnady, C. "Present Day Kinematics of the East African Rift." *Journal of Geophysical Research: Solid Earth* 119, no. 4 (2014): 3584-600.
- Scholz, C., Cohen, A., Johnson, T., King, J., Talbot, M., and Brown, E. "Scientific Drilling in the Great Rift Valley: The 2005 Lake Malawi Scientific Drilling Project—an Overview of the Past 145,000 Years of Climate Variability in Southern Hemisphere East Africa." *Palaeogeography, Palaeoclimatology, Palaeoecology* 303, no. 1-4 (2011): 3-19.
- Siler, D. L., and Faulds, J. E. "Three-Dimensional Geothermal Fairway Mapping: Examples from the Western Great Basin, USA." *Geothermal Resources Council, Davis, CA (United States)*, (2013).
- Van der Beek, P., Mbede, E., Andriessen, P., and Delvaux, D. "Denudation History of the Malawi and Rukwa Rift Flanks (East African Rift System) from Apatite Fission Track Thermochronology." *Journal of African Earth Sciences* 26, no. 3 (1998): 363-85.
- Versfelt, J., and Rosendahl, B. "Relationships between Pre-Rift Structure and Rift Architecture in Lakes Tanganyika and Malawi, East Africa." *Nature* 337, no. 6205 (1989): 354.
- Von Herzen, R.P., and Vacquier, V. "Terrestrial Heat Flow in Lake Malawi, Africa." *Journal of Geophysical Research* 72, no. 16 (1967): 4221-26.
- Wang, T., Feng, J., Liu, K. H., and Gao, S. S. "Crustal Structure beneath the Malawi and Luangwa Rift Zones and Adjacent Areas from Ambient Noise Tomography." *Gondwana Research* 67 (2019): 187-98.
- Wheeler, W. H., and Karson, J. A. "Structure and Kinematics of the Livingstone Mountains Border Fault Zone, Nyasa (Malawi) Rift, Southwestern Tanzania." *Journal of African Earth Sciences (and the Middle East)* 8, no. 2-4 (1989): 393-413.